Available online at www.sciencedirect.com
ScienceDirect
Coordination Chemistry Reviews 252 (2008) 2156–2170
COORDINATION CHEMISTRY REVIEWS
www.elsevier.com/locate/ccr

Review

^{31}P and ^{13}C NMR studies on metal complexes of phosphorus-donors: Recognizing surprises

Paul S. Pregosin *

Laboratory of Inorganic Chemistry, ETHZ, 8093 Zürich, Switzerland

Received 20 June 2007; accepted 30 January 2008
Available online 8 February 2008

Contents

Abstract

^{31}P and ^{13}C NMR methods are shown to provide the necessary clues to understand the unexpected and often very novel reactions of a series of ruthenium and palladium phosphine complexes based on the chiral biaryl-based phosphine auxiliaries BINAP, MeO-Biphep and MOP. Many of these reactions involve complexation of seemingly remote olefin moieties and subsequent P–C bond cleavage.

Keywords: ^{31}P and ^{13}C NMR; Biaryl phosphines; Ru and Pd-olefin and arene complexation; P–C bond cleavage

1. Introduction

Phosphine complexes continue to enjoy immense popularity in connection with homogenous catalysis and organometallic chemistry. In the field of enantioselective catalysis dozens of chiral phosphine auxiliaries are in use and many of these are commercially available, e.g. various BINAP products.

Multinuclear NMR spectroscopy and especially ^{31}P NMR [1], has been a major contributor to the synthesis of new phosphorus containing compounds and complexes (e.g., via routine ^{31}P NMR screening) as well as to our understanding of the structures and reactivity of these species. In the course of preparing a rather large number of Ru and/or Pd-complexes containing BINAP, **1**, MeO-Biphep, **2**, the MOP class, **3**; and other aryl phosphine or phosphoramidite derivatives, e.g., phosphoramidite **4**, we have developed a "standard" NMR approach in the recognition of both gross and fine structural details when the problem does not fall into a routine category. Apart from obtaining conventional ^{31}P and ^{13}C spectra, this approach involves routinely measuring 2D ^{31}P,^{1}H and, ^{13}C,^{1}H one-and multiple bond-spectral correlations.

* Tel.: +41 44 6322915; fax: +41 44 6331071.
E-mail address: pregosin@inorg.chem.ethz.ch.

0010-8545/$ – see front matter © 2008 Elsevier B.V. All rights reserved.
doi:10.1016/j.ccr.2008.01.035

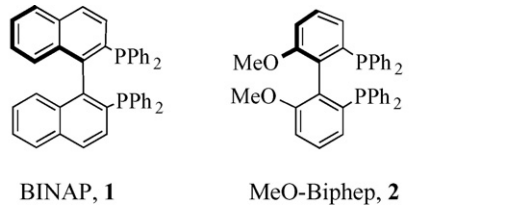

BINAP, **1** MeO-Biphep, **2**

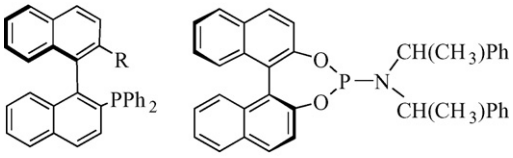

MOP class, **3** Phosphoramidite, **4**

Using these NMR methods we have come across of number of unexpected reactions based on olefin and arene bonding, which have led to the development of interesting new Ru and Pd-chemistry. This perspective is designed to highlight aspects of these reactions while simultaneously demonstrating how these ^{31}P and ^{13}C NMR methods have contributed to the development of this chemistry. Of course various forms of Overhauser spectroscopy can be equally valuable; however, these methods have been discussed, in detail, elsewhere [2].

2. ^{31}P NMR

^{31}P{^{1}H} NMR spectroscopy is so attractive because the large chemical shift range [1,3] together with the sensitivity of the shift to structural change allows one to determine, often just by inspection, if a reaction has taken place. In the majority of molecules one observes only a single resonance. When more complicated ^{31}P spin systems are present the ^{x}J(^{31}P,^{31}P) values usually provide additional essential clues with respect to the structure(s) that arise [4]. Occasionally the ^{31}P chemical shift, by itself, is informative and the following examples from ruthenium chemistry are illustrative.

The reaction of [RuH(BINAP)(η^6-benzene)]OTf with PPh_3 in 1,2-dichloroethane

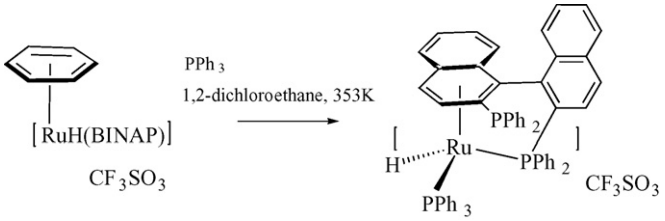

6 (1)

at 353 K affords a single product, **6**, in high yield [5]. The ^{31}P spectrum of the crystallized product (Fig. 1) revealed three signals centered at 59.5, 47.7 and −14.3 ppm. The two high frequency signals reveal ^{2}J(^{31}P,^{31}P) coupling, whereas the low frequency resonance appears as a singlet. Based on these data, it seemed one of the three P-atoms was not complexed. ^{1}H NMR showed the presence of a single hydride ligand and the ^{13}C data confirmed the η^6-BINAP arene (more on this point later). A

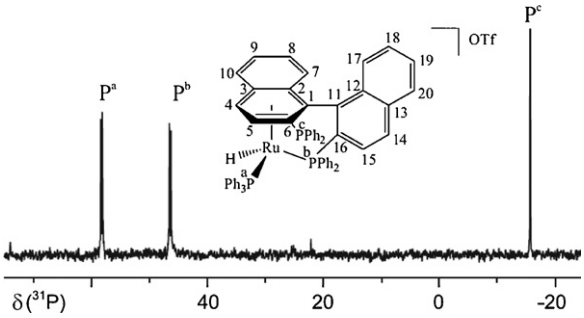

Fig. 1. The ^{31}P NMR spectrum of salt **6**, showing the three non-equivalent NMR signals [5].

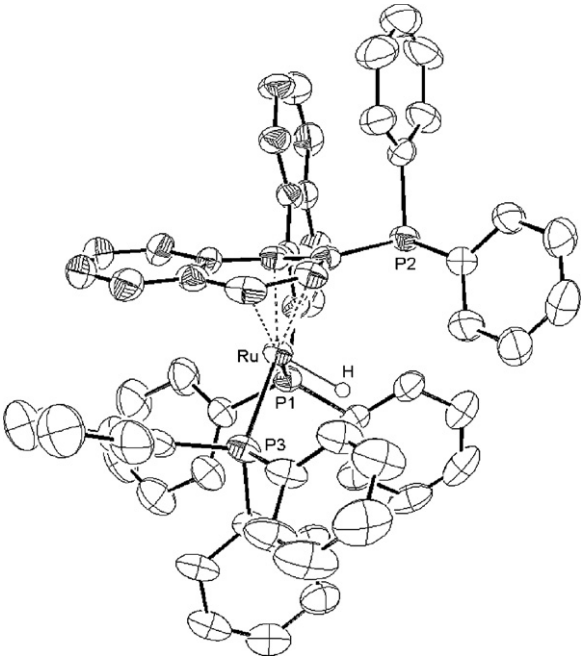

Fig. 2. The solid-state structure of **6** with P2 and P3 (but not P1) complexed [5].

^{31}P,^{1}H correlation indicated that the ^{31}P-signal at low frequency was associated with the BINAP protons (and not the PPh_3), and eventually a solid-state structure (Fig. 2) rounded off the picture. With three good donors, the Ru(II)-atom prefers to complete the coordination sphere with the arene. Three σ-donor ligands (the hydride and two P-atoms) are complemented by the π-acceptor η^6-arene thus affording a stable 18e species. This leaves one P-donor "dangling".

Reaction of the substituted $Ru(OAc)_2$(MeO-Biphep) complex (see Eq. (2))

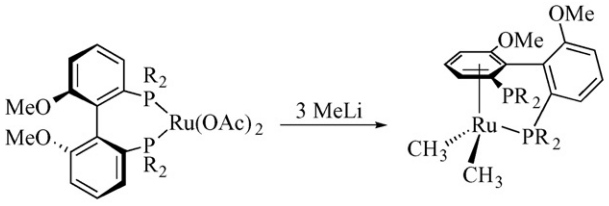

7 R = 3,5-di *t*-Bu phenyl (2)

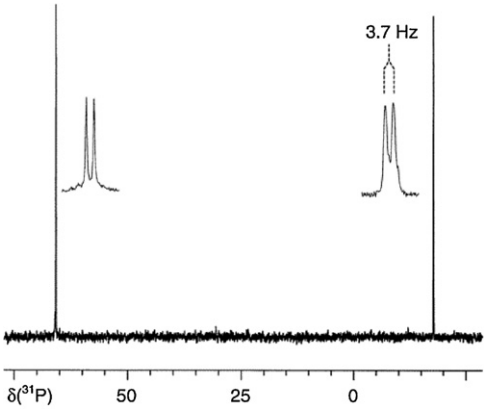

Fig. 3. ^{31}P NMR spectrum of **7** (162 MHz, CD_2Cl_2).

with methyl lithium resulted in somewhat related chemistry [6]. The product, **7**, obtained in >90% yield, revealed an unexpected ^{31}P NMR spectrum (see Fig. 3). Again, one observes a low-frequency ^{31}P signal, typical of an uncomplexed P donor. In this case a small spin–spin coupling of 3.7 Hz connects the two P-nuclei. The ^{1}H NMR spectrum showed the two Ru-methyl groups and the ^{13}C data confirmed the presence of an η^6-arene fragment. Fig. 4 shows the ^{13}C,^{1}H one-bond correlation and reveals the three arene CH carbon signals (C3–C5), between ca. 70 and 100 ppm, shifted to markedly lower frequency as a consequence of the arene complexation. This ^{13}C coordination chemical shift is diagnostic for arene complexation [7]. Here, as well, three good donors (the two Ru-methyl groups and one P-atom) are combined with the η^6-arene, with the result that one P-atom is left free.

Sometimes it is sufficient to have a single diagnostic ^{31}P chemical shift. The reaction of $[Ru(Cp^*)(CH_3CN)_3](PF_6)$ with the very bulky tri-*o*-tolyl phosphine resulted in a ^{31}P NMR spectrum with a singlet at $\delta = -36.7$(!) [8]. This chemical shift which appears at an unusually low frequency, is not consistent with P-coordination, and thus provides an indication of the formation of the unexpected product, $[Ru(Cp^*)\{(\eta^6\text{-}o\text{-tolyl})P(o\text{-tolyl})_2\}](PF_6)$, **8**, in which the P-atom is not coordinated. This η^6-*o*-tolyl complex could be isolated in good yield (see Eq. (3)) as a yellow powder, and both the

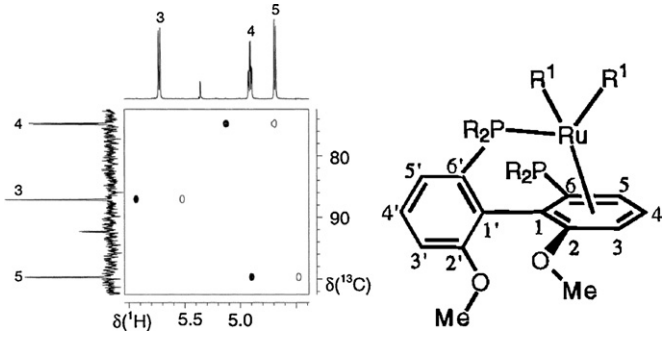

Fig. 4. The ^{13}C,^{1}H one-bond correlation for **7** showing the three arene CH carbon signals (C3–C5). R^1 = Me [6].

^{13}C and solid-state diffraction data confirm the proposed structure [8].

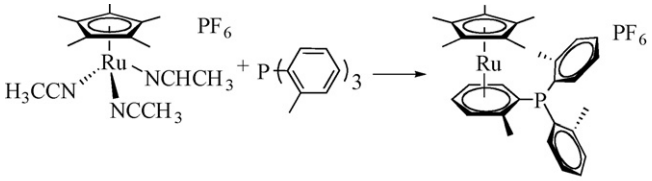

8 (3)

3. ^{13}C NMR and olefin complexation

Yet another unexpected ^{31}P chemical shift lead us into the olefin complexation chemistry of BINAP and MeO-Biphep. In connection with a collaboration with colleagues in the Roche laboratories in Basel [9], we allowed a Ru(MeO-Biphep) complex, R = i-Pr, to react with 1,5-COD and HBF_4 (see Eq. (4)).

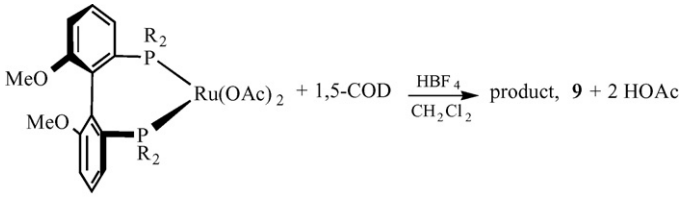

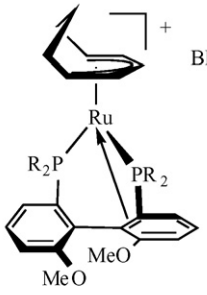

9 R = i-Pr (4)

The ^{31}P NMR spectrum of the product, **9**, gave an AX spin system; however, one of the two phosphorus chemical shifts (69.6 and −11.2 ppm) appeared at low frequency (indeed not far from the signals shown in Figs. 1 and 2). Although this chemical shift might be thought to be associated with uncoordinated phosphine, this was *not* the case.

The fate of the complexed 1,5-COD organometallic ligand was not immediately obvious; however, a one-bond ^{13}C,^{1}H-correlation, for **9**, showed only three aliphatic CH_2 type signals, but *five* CH-absorptions in the region 57–114 ppm. These ^{13}C chemical shift data were strongly suggestive of the cyclo-octapentadienyl fragment, $Ru(\eta^5\text{-}C_8H_{11})$ [10]. Further, a long range ^{13}C,^{1}H HMQC correlation revealed two *non-protonated* ^{13}C resonances at 74.5 ppm, as a doublet, and 95.1 ppm, as a triplet, These carbons are coupled to protons from one of the two MeO-Biphep biaryl rings as indicated in fragment **10** (a ^{1}H,^{1}H

COSY helped to assign the two three-spins systems). The ^{13}C signals for the corresponding carbons of the second biaryl ring, C(1′), 139.7 ppm and C(6′), 135.4 ppm, were found at normal higher frequency. The relatively low frequency positions of these two carbon resonances suggested that the remote C(1)–C(6) biaryl double-bond is coordinated to the metal, thereby affording an 18e complex, and thus making the MeO-Biphep ligand a six-electron donor to the metal. It should be emphasized that this type of olefin bonding would have gone unnoticed for a longer period if it were not for the long-range $^{13}C,^{1}H$ HMQC spectrum, which readily allows the assignment of fully substituted ^{13}C signals [11].

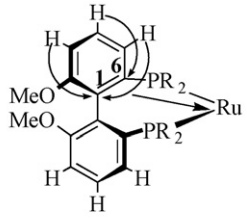

10 δC(1) =9 5.1, δ C(6) = 74.5

The low frequency ^{31}P signal at −11.2 ppm in **9** *is* associated with a complexed P-donor and results from the unexpected four-membered ring coordination mode. Clearly, not every low frequency ^{31}P resonance can be assigned to a "free" donor. We have subsequently prepared a large number of such olefin complexes (and documented their solid-state structures, e.g., as shown in Fig. 5 for Ru(Cp)(MeO-Biphep)$^+$, **11** [12]).

The recent literature reveals a few more related interactions [13–17] (see Scheme 1 for **12–16**). However, White and co-workers [18], who reported on Ru(Cp)(BINAP)$^+$, **17**, must be credited with the first report of this type of bond in a complex.

Given the η^2-olefin complexation it is not surprising that the aromaticity in that ring is lost. The relevant X-ray data, for **9**, show that the C3–C4 and C5–C6 separations, ca. 1.35–1.36 Å, are now indicative of localized double bonds [9].

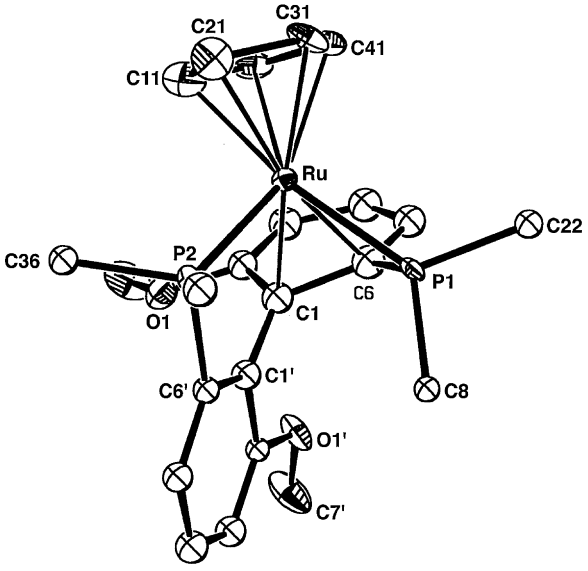

Fig. 5. The solid-state structure of the cation Ru(Cp)(MeO-Biphep)$^+$, **11** [12].

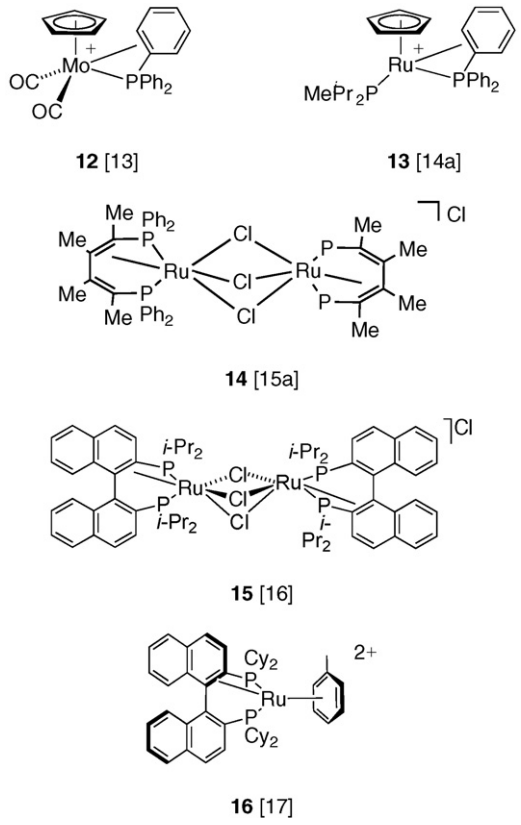

12 [13] **13** [14a]

14 [15a]

15 [16]

16 [17]

Scheme 1. Examples showing the remote olefin bonding.

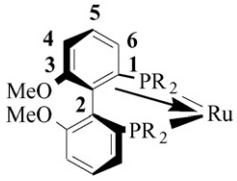

C(1)-C(2) = 1.453(7)
C(2)-C(3) = 1.430(7)
C(3)-C(4) = 1.362(8)
C(4)-C(5) = 1.410(9)
C(5)-C(6) = 1.354(9)
C(1)-C(6) = 1.409(7)

9

Table 1 shows ^{13}C and ^{31}P data for a set of BINAP and MeO-Biphep arene complexes that show this type of 6e donor character [19].

4. An extension to MOP

Once it is recognized that the biaryl fragment is not always "innocent" with respect to its bonding characteristics, one can begin to imagine (and search for) new and related complexation modes in biaryl-based ligands. The monodentate auxiliary, MOP, prepared and studied by Hayashi and co-workers [20–23], provides a natural extension of this type of olefin coordination. The stable dinuclear Pd(I) salt, **21**; contains a bridging diene moiety which uses a part of the MOP biaryl backbone for the complexation [24]. Each Pd-atom complexes *one* double bond. The ^{31}P data are fairly routine, however, the ^{13}C data for **21** reveal the two fully substituted carbons at low-frequency positions, due to the complexation: C1 (99.7 ppm) and C6 (136.7 ppm), plus the two =CH carbons, C4 (85.0 ppm) and C5 (79.4 ppm). The latter two chemical shifts can be seen in Fig. 6.

In Pd(I) dinuclear chemistry, this type of bridging behaviour has been recognized, e.g., **22** [25], and **23** [26], and even more so in the recent compounds reported by Murahashi and Kurosawa [27,28].

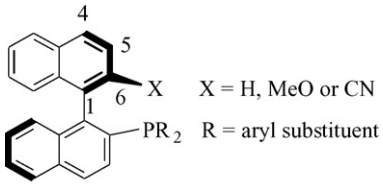

MOP ligands, **20**

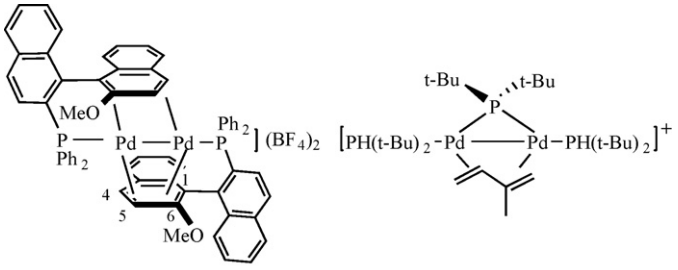

21 **22**

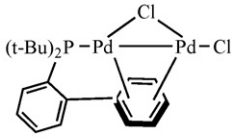

23

The acetyl acetonate Pd-complexes, **24** and **25**, derived from the HO and MeO-MOP ligands, are very interesting [29]. Neutral complex **24**, was obtained directly from $Pd(acac)_2$ by adding HO-MOP, whereas cationic **25** was prepared starting from $[Pd(acac)(CH_3CN)_2]BF_4$ and adding MeO-MOP. In **24**, the hydroxyl function has lost a proton to afford a keto-anionic chelating ligand.

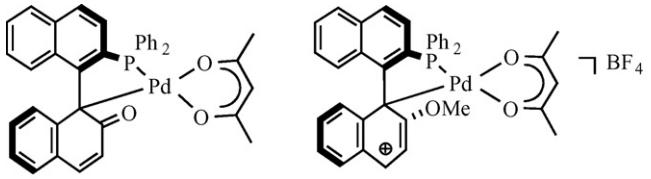

24 **25**

The ^{31}P chemical shifts for **24** and **25**, $\delta = 46.5$ and 48.5, respectively, appear at considerably higher frequency than for the routine *trans*-$PdCl_2(MOP)_2$ types and are suggestive of the known "ring effect" [30], on the ^{31}P chemical shift that results from the formation of five-membered rings.

The $^{13}C,^{1}H$ long-range correlations again provide the key assignments for the fully substituted carbon resonances directly bound to the Pd-atoms (see Fig. 7). For both **24** and **25** the ipso carbons, C1, involved in the Pd-bonding,

Table 1
Selected ^{13}C and ^{31}P NMR data for the Ru-BINAP and MeO-Biphep arene complexes **18** and **19**

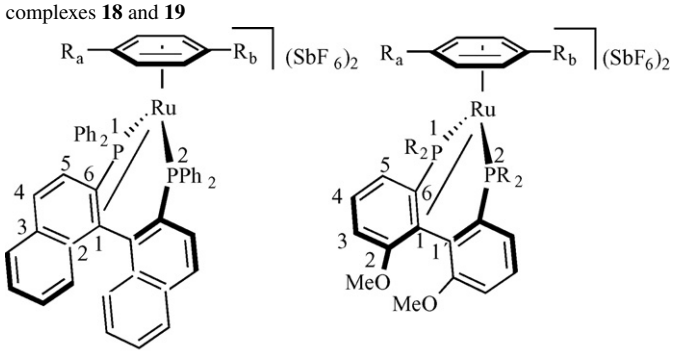

18a, **19a** **18b** (R=Ph), **18c** (R=iPr) and **19b** (R=Ph)

18, p-cymene = R_a=CH_3, R_b=$CH(CH_3)_2$
19, benzene = R_a=H, R_b=H

Complex	$^{13}C1$	$^{13}C6$	$^{31}P1$	$^{31}P2$
18a	98.0	67.5	3.3	68.7
18b	93.0	80.1	7.7	67.1
18c	102.5	79.1	27.3	82.6
19a	101.7	73.0	19.0	64.0
19b	90.9	86.0	15.4	64.7

BINAP and MeO-Biphep complexes of Ru(II) [19].

appear at lower frequency, $\delta = 70.5$ and 86.7, respectively. For **25**, one can also use the three-bond coupling constant, from the protons of the methoxy group, ^{3}J(C6, H(MeO)) to confirm the assignment of C6 [29] (see **20** for the numbering).

As indicated in Fig. 7, the ketonic carbon in **24**, at $\delta = 193.7$, is readily observed and found at a much higher

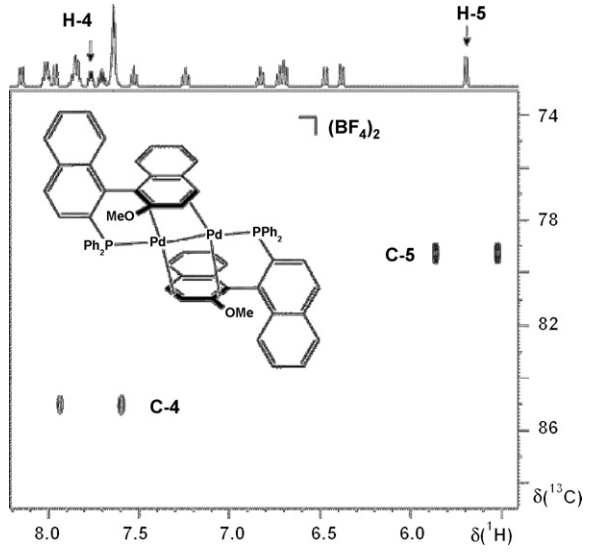

Fig. 6. $^{13}C,^{1}H$ one-bond correlation for the MeO-MOP complex, **21**. The two carbon signals for C4 (85.0 ppm) and C5 (79.4 ppm) appear at typical low-frequency positions (see **20** for numbering) [24].

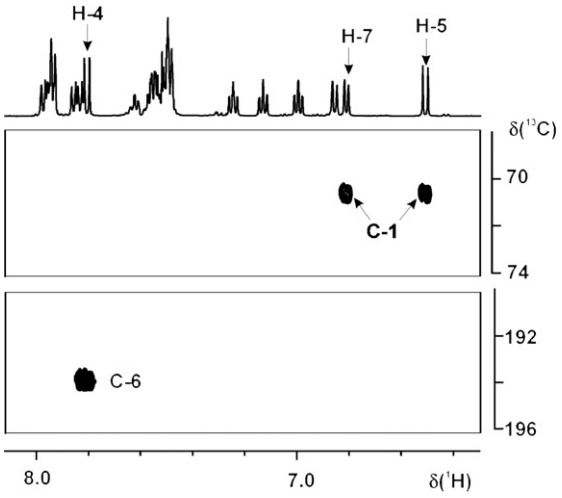

Fig. 7. $^{13}C,^{1}H$ long-range correlation for **24** showing the fully substituted carbon at $\delta = 70.5$, as well as the ketonic carbon at $\delta = 193.7$ [29].

frequency than one would expect for a phenolic sp^2 carbon. Moreover, the organic ^{13}C NMR literature suggests that this is exactly the correct δ value for the carbonyl of an α,β-unsaturated ketone [31]. Several analogous Pt-complexes [32], have also been reported and the various values of $^{1}J(^{195}Pt,^{13}C)$ help in understanding how the metal–atom bonds to these MOP carbons. The charge distribution in the cation **25** is not obvious; however, the coordination chemical shifts, indicated below, suggest that the positive charge in **25** is spread across alternating carbons in both of the naphthyl rings [29].

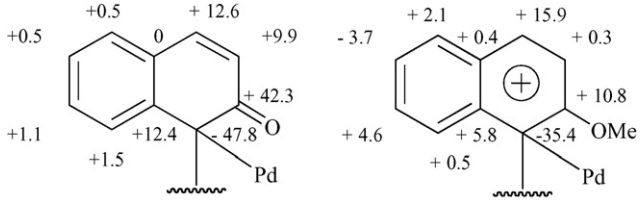

^{13}C coordination chemical shifts for

24 and **25**

The solid-state structures for cationic **24** and neutral **25** were determined via X-ray diffraction methods (see Fig. 8) and confirm that both structures contain Pd–C σ-bonds arising from the MOP naphthyl backbone [29]. As expected, based on the relative positions of the two ^{13}C C1 resonances, **24**, possesses the shorter Pd–C bond length.

Slowly, subtle but related variations on these bonding modes are emerging. Chauvin and co-workers [33], have found a *diene mode* of bonding in the Rh-cation, **26**, and, in a series of papers Kocovsky, Lloyd-Jones and co-workers [34,35] have found that "MAP" (the NMe_2 analog of MeO-MOP) can also form a sigma bond from the ipso carbon to palladium, as in **27**.

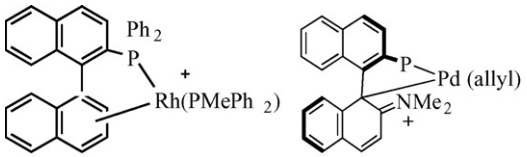

26 **27**

It is interesting that the now well-known binol-based phosphoramidite ligands do not (to-date) show this type of biaryl olefin bonding when complexed. However, they do reveal P,(olefin) chelate-type behaviour in that they are capable of complexing a pendant aryl ring in an η^2 fashion, e.g., as in the Ru-complexes **28** and **29** [36]. Once again the long-range $^{13}C,^{1}H$ correlation helps to secure the solution structure (see Fig. 9). The coordination chemical shifts for C1 and C2 are not quite so large, as in the previous examples, but nevertheless, these are consistent with the proposed bonding mode.

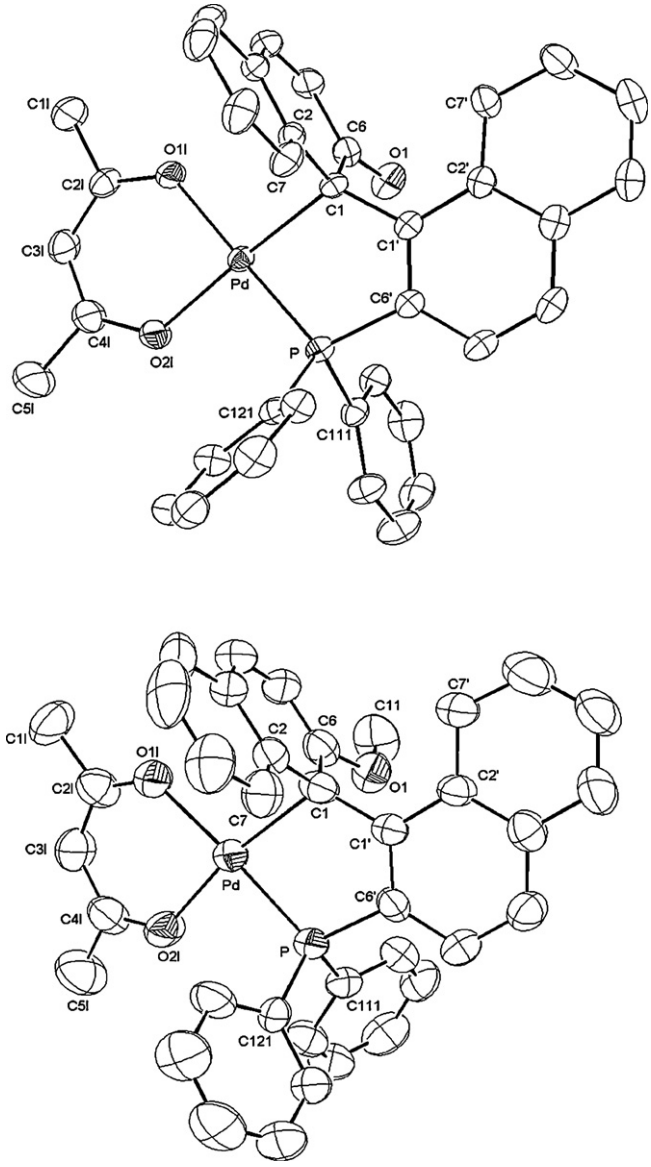

Fig. 8. The solid-state structures **24** (top) and **25** (bottom) [29].

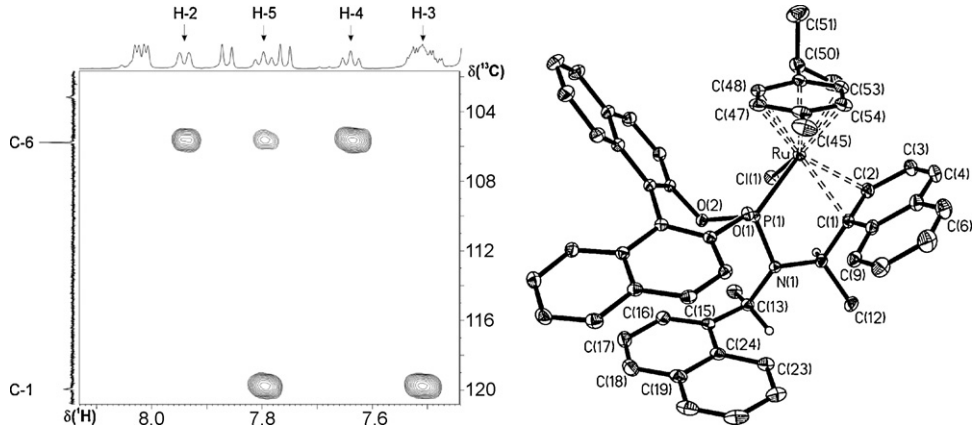

Fig. 9. (left) ^{13}C–^{1}H long-range correlation from a heteronuclear multibond correlation (HMBC) spectrum of **29** and (right) *ORTEP plot of* (S_a, S_{Ru}, R_C, R_C)-**29**. The two carbons on the vertical axis are C1 and C2 (not C6).

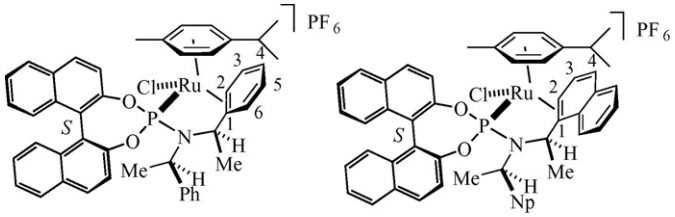

28 **29**

Summarizing, it is clear that for the BINAP, MeO-Biphep and MOP structural types, the backbone biaryl π-system can become involved in the bonding. It may appear that some of the double bonds are remote from the metal center; nevertheless, the late transition metals have no trouble in accessing these electrons. ^{31}P and especially ^{13}C NMR data are important for the proper characterization of these species in solution.

5. P,C bond cleavages and ^{31}P,^{1}H correlations

Reaction of either the $Ru(OAc)_2$(MeO-Biphep) complex, **30** [37] (or the analogous BINAP complex, **31** [17]) with wet HBF_4 leads to the exotic O–$B(F)_2$–O–P chelate complexes, **32** and **33**, as indicated in Scheme 2. These complexes each contain an H-bonded HBF_4 molecule. These two rather unusual species (for which there exist solid-state structures) arise from a series of reactions.

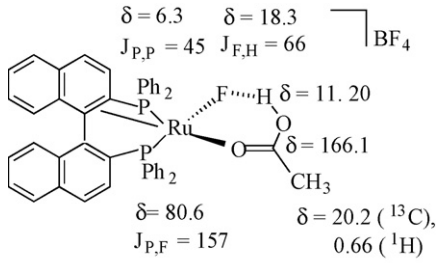

34

Via low temperature NMR, it can be shown that, immediately after the addition of acid, one acetate ligand has been protonated and removed. One of the intermediates, **34**, can be characterized [38]. A fluoride has been extracted from the HBF_4 and this

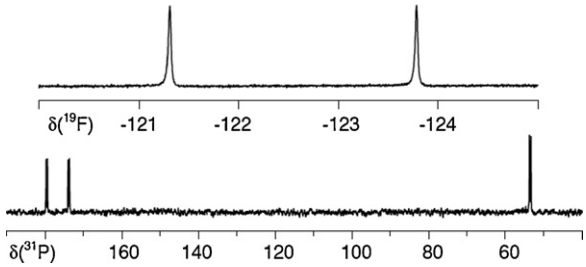

Fig. 10. The ^{19}F and ^{31}P spectra for **35b**. The large $^{1}J(^{31}P,^{19}F)$ value is diagnostic of a P–F bond [38].

new salt contains a weak Ru–F bond, and not a coordinated HF molecule. The magnitude of the value $^{1}J(^{19}F,^{1}H)$, 66 Hz, is diagnostic and is much too small to be associated with a direct H–F bond [38]. Note the low frequency ^{31}P chemical shift, 6.3 ppm for one of the P-donors and the complexed double bond! This small ring strained species cleaves a P–C bond to afford **35a** (as a mixture of two components) that can be characterized, but is not stable at room temperature. Structure **35a** represents the net result from the addition of HF across a P–C bond, although this is not necessarily the mechanism. Reaction of **35a** with excess chloride affords the stable, isolable, **35b**, in good yield (see Eq. (6) and Fig. 10). The clearly resolved, large $^{1}J(^{31}P,^{19}F)$ value of >900 Hz is typical for a P–F bond [38]. The intermediate **35a** represents the species that reacts with the BF_2O_2 anion from the hydrolysed BF_4^-, to afford the observed product which contains the P–O–B(F_2)–O chelate ring.

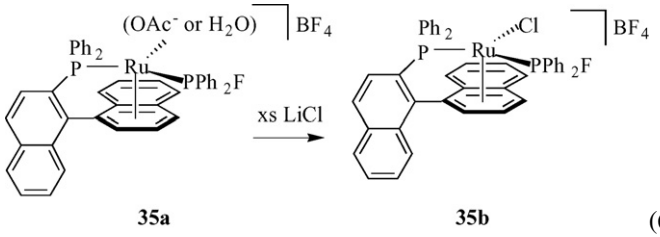

35a **35b** (6)

Part of the chemical complexity (that due the hydrolysed BF_4^-) can be eliminated via the use of triflic acid, HOTf instead of HBF_4 (see Scheme 3); however, the intermediates and products which result, are not trivial. Warming the neutral bis-acetate

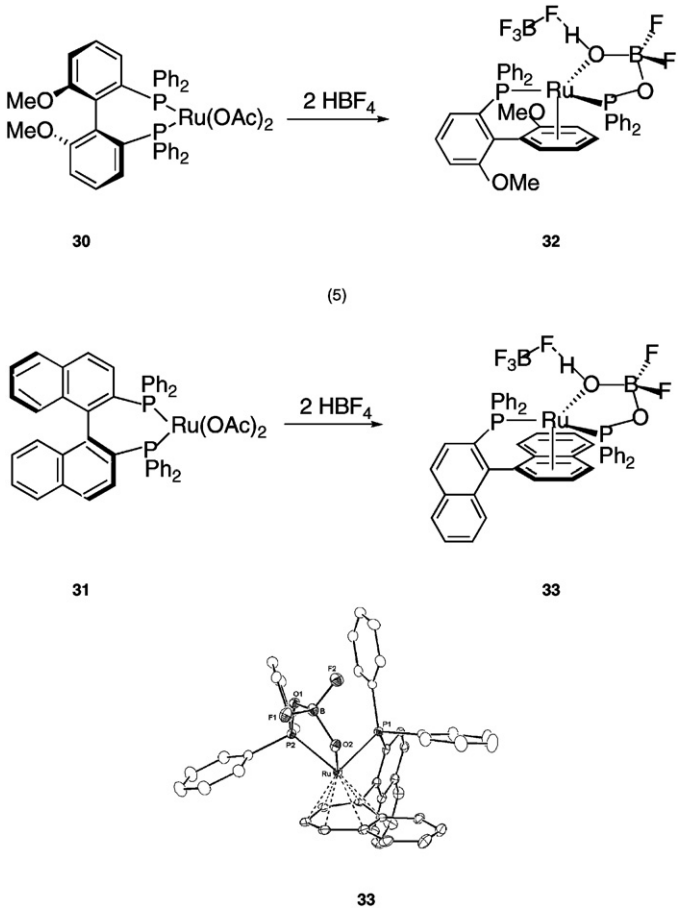

Scheme 2. The P–C bond cleavage products **32** and **33** and a view of the structure of **33**.

with HOTf in 1,2-dichloroethane at 353 K leads to a rapid regioselective cleavage of one of the P–C bonds. The first easily isolable product is arene complex, **36** [38]. This shows an AX ^{31}P spectrum in which one of the signals has a relatively high frequency ^{31}P chemical shift, ca. 114 ppm, suggesting the presence of an electronegative group on the P-atom.

Superficially, salt **36** appears to result from the addition of water across the P–C bond. Partially, the water comes from the triflic acid. However, an independent experiment using a ^{13}C enriched Ru-acetate complex (see Scheme 4 and Fig. 11) reveals that *acetic anhydride and water* are produced in this reaction [39]! The new Ru-product reveals a ^{31}P signal at >185 ppm. This chemical shift is suggestive of the presence of oxygen on phosphorus but, most likely, within a five-membered chelate ring given that the coordinated P(OH)Ph$_2$ ligand in **36** appears around 114 ppm. The product, **39**, which has the structure shown in the lower right hand corner of Scheme 4, can be isolated [16,39]. Further, as indicated in the scheme, **39** reacts with water to give the initially isolated Ru-P(OH)Ph$_2$ complex, **36**. The metallated species in the center of Scheme 4 is postulated but not proven. Fig. 12 shows views of the structure of the P(cyclohexyl)$_2$ analog (instead of PPh$_2$) version of **39**.

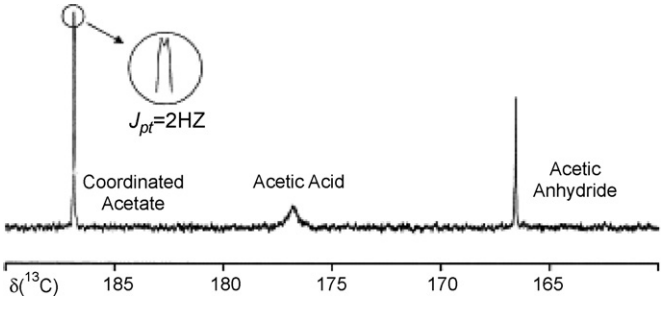

Fig. 11. The ^{13}C NMR spectrum recorded after warming the solution for 30 min at 353 K. The peaks for complexed acetate, acetic acid and acetic anhydride are indicated. The expanded section shows the P, C coupling, ^{2}J = 2 Hz (75 MHz, 1,2-dichloroethane with D$_2$O capillary as internal lock) [39].

Subsequent reaction of **36** with methanol and other alcohols leads to the complexes **37**, as indicated in Fig. 13 and Eq. (7) [40]. Further reaction with water affords **38**.

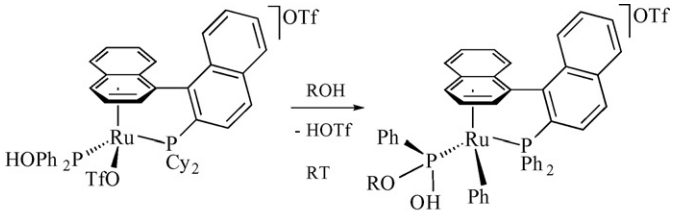

36 **37** R = a) Me, b) Et, c) i-Pr (7)

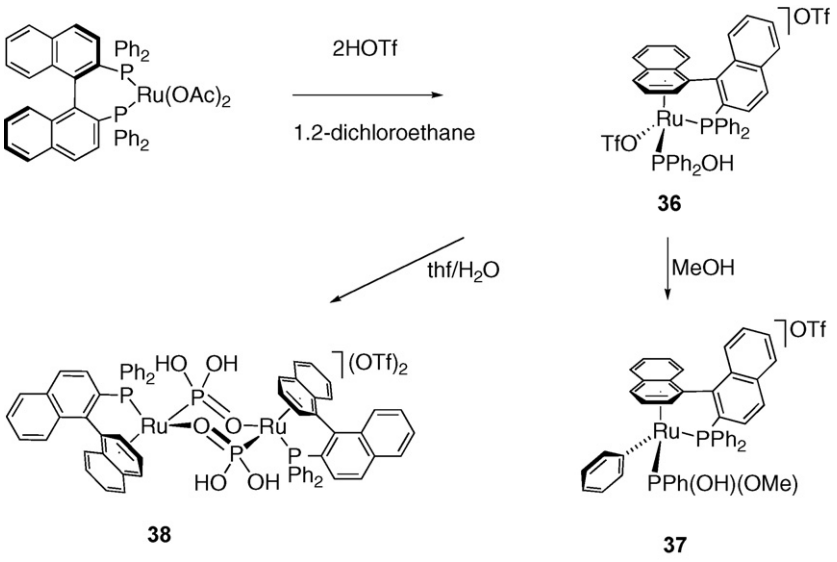

Scheme 3. Related P–C bond cleavage chemistry starting from triflic acid.

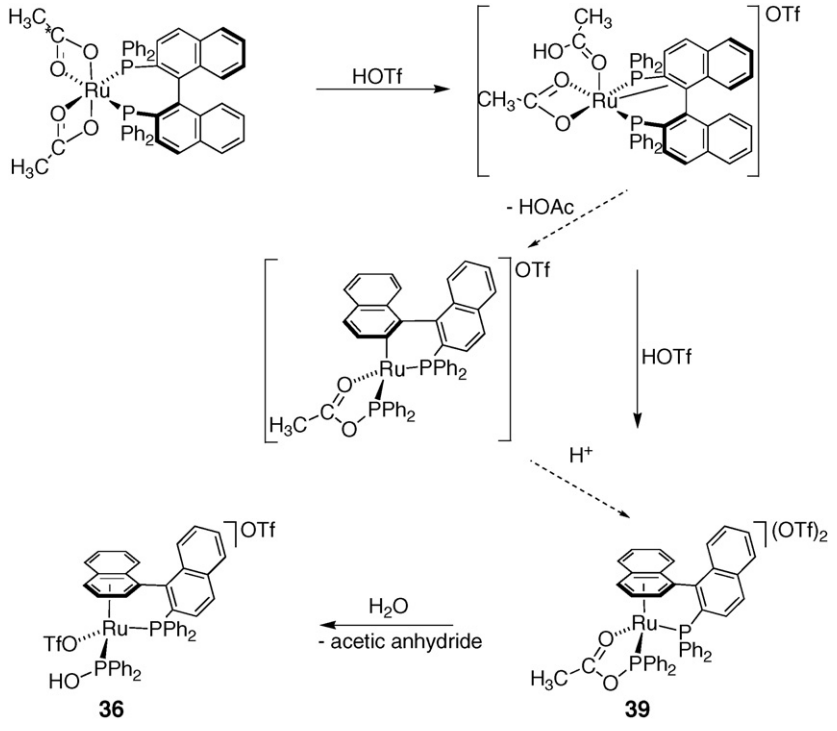

Scheme 4. Intermediates in the $Ru(OAc)_2$(BINAP) triflic acid chemistry.

The hydrolysis product **38** [41] represents the first example of a phosphorus acid ligand functioning as a P (rather than an O) donor and demonstrates a clear chair-like $(P–O)_3$ six membered ring (Fig. 14).

As part of the structural analyses for the arene complexes **36**–**38** it was useful to assign the *ortho* protons of the P-phenyl rings. Fig. 15 shows the high frequency section of the $^{31}P,^{1}H$ correlation for compound **36** [38]. The correlation to the high frequency OH proton is clear, as are the *two strong sets of cross-peaks due to the two kinds of ortho P-phenyl protons* (each with relative integral = 2). Further, there are weaker correlations to naphthyl backbone and *meta* protons and to one of the protons of the complexed arene ring.

Fig. 16 (top) gives a slice through the $^{31}P,^{1}H$ correlation (for the high frequency resonance at $\delta = 142.4$ [40]) for **37b** showing only *one set of strong cross-peaks from the ortho protons of the remaining P-phenyl ring*, ca. 6.6 ppm. In addition, one sees the two non-equivalent methylene protons of the ethoxy-group as

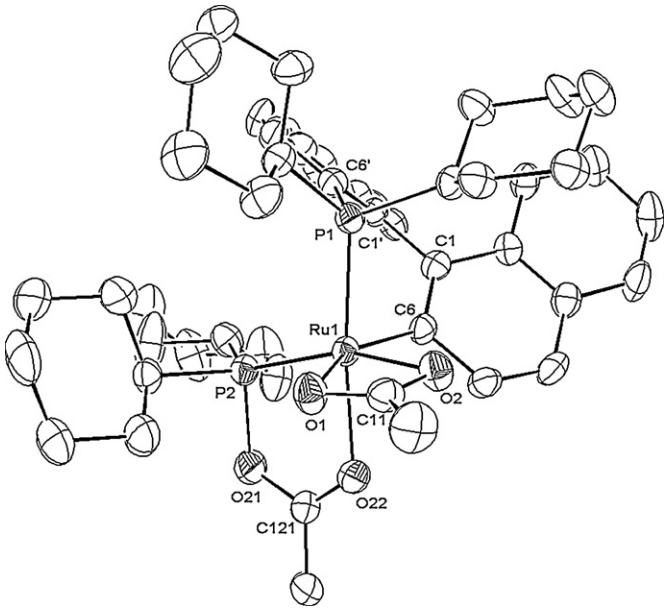

Fig. 12. View of the solid-state structure of the P-cyclohexyl version of **39** [16].

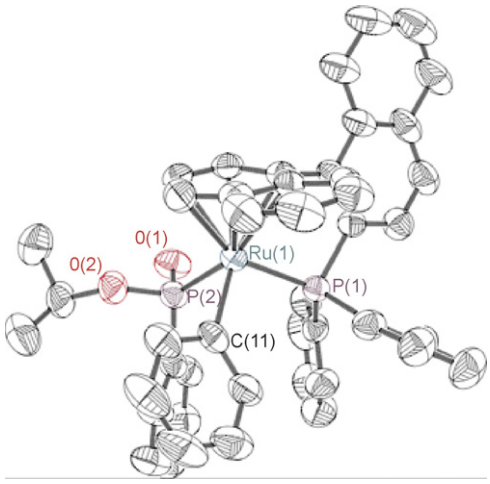

Fig. 13. The solid-state structure of **37c** with R = i-Pr [4].

multiplets (one of which is almost completely covered by the THF-d_8 OCH_2 of the solvent). Fig. 16 (bottom) gives the $^{31}P,^{1}H$ correlation for **38**. For the high frequency ^{31}P resonance one finds *only* cross-peaks to the two diastereotopic P(OH) groups (all the phenyls are gone [41]). The low frequency ^{31}P signal reveals the expected cross-peaks to the two P-phenyl *ortho* protons from the remaining PPh_2 group. Thus careful application of this P,H-methodology allows us to keep track of the number of P–C cleavage reactions.

6. An HMQC excursion: technical bits and pieces

Both ^{31}P HMQC and ^{13}C HMQC spectra have been indispensable in this area of phosphorus chemistry. Nevertheless, with respect to phosphorus-proton correlations, it is useful to distinguish between $^{31}P,^{1}H$-COSY and $^{31}P,^{1}H$ HMQC type measurements.

In general, the HMQC approach is especially useful for finding correlations to nuclei with small magnetic moments and is the recommended method for determining ^{103}Rh and ^{183}W chemical shifts amongst many others [42–46]. Occasionally one experiences problems [45]; nevertheless, this approach is favored since the gain in signal-to-noise (relative to conventional methods), represents several orders of magnitude [42].

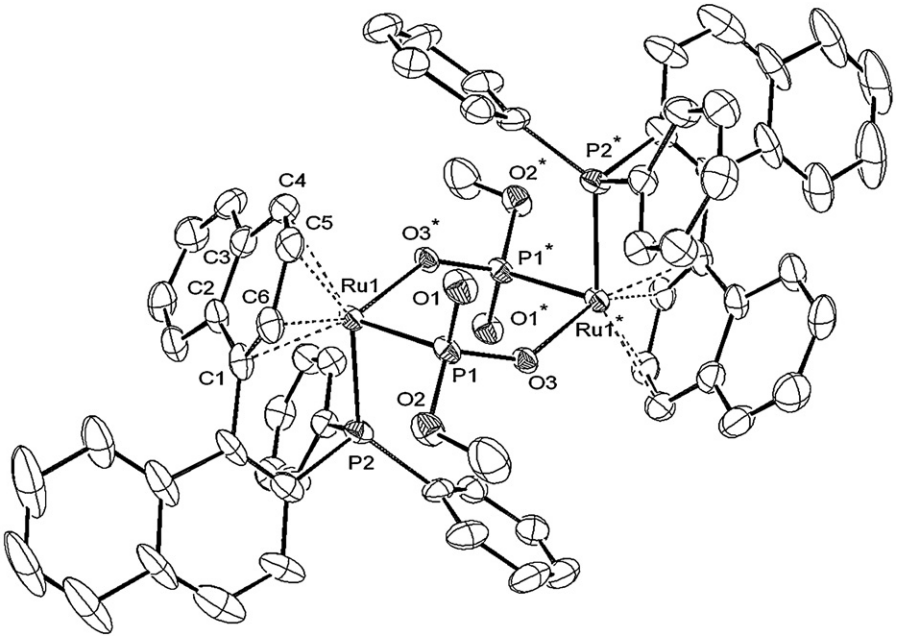

Fig. 14. The solid-state structure **38** showing the flattened chair conformation of the six-membered ring [41].

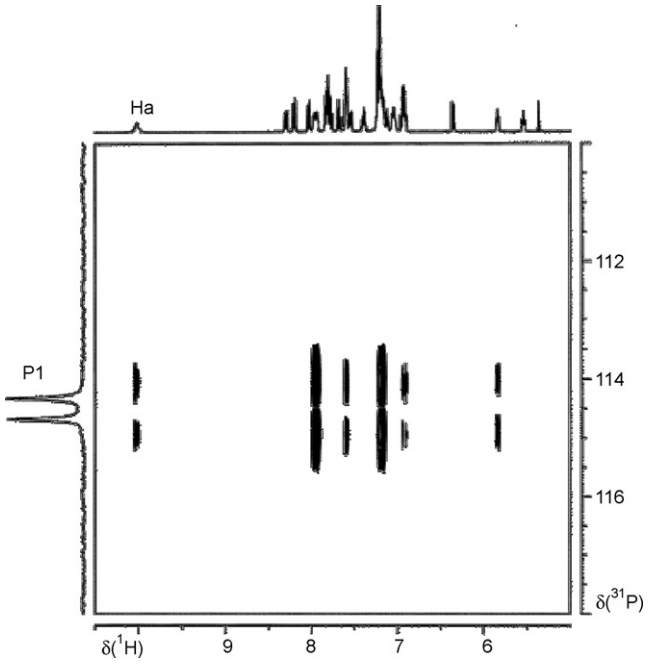

Fig. 15. High frequency section of the $^{31}P,^{1}H$ correlation belonging to compound **36** (400 MHz, CD_2Cl_2, ambient temperature) [38].

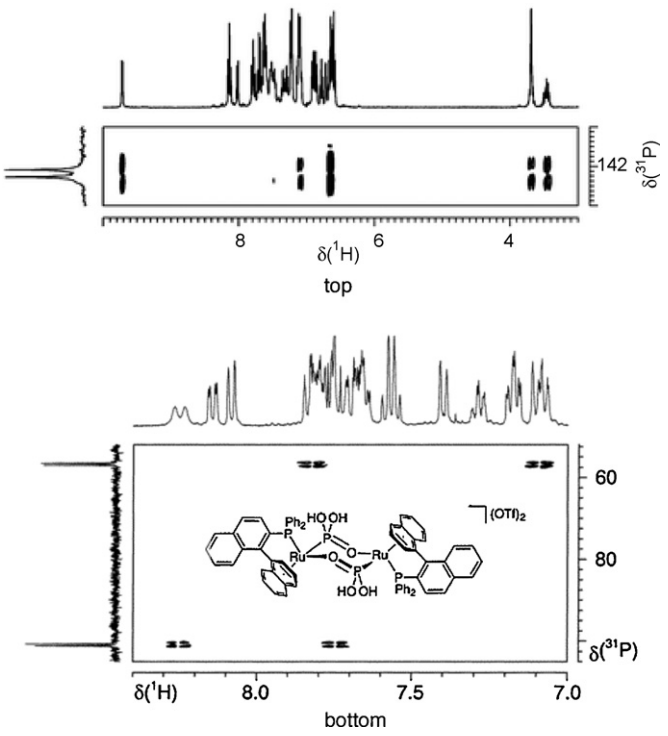

Fig. 16. (top) Slice through the ^{31}P–^{1}H correlation for **37b** ($\delta = 142.4$) showing only *one* set of strong cross-peaks from the *ortho* protons of the remaining P-phenyl ring, ca. 6.6 ppm, plus the hydroxy P(OH), at high frequency [40]. (bottom) The $^{31}P,^{1}H$ correlation for **38** showing (a) *only* cross-peaks to the two diastereotopic P(OH) groups (all the phenyls are gone) and (b) the expected cross-peaks to the two P-phenyl *ortho* protons [41].

For these metal nuclei the magnitudes of the spin–spin coupling constants to protons are modest (and often unknown). Since one needs to input an estimate of this coupling constant (the waiting time called "Δ" in the pulse sequence is equal to (1/2)*J*, where *J* is this coupling constant, see Fig. 17a), one often makes an "educated guess" with respect to its magnitude. The following two examples are now fairly typical.

Fig. 18 shows the $^{103}Rh,^{1}H$ correlation for the unrelated salt **40** [47]. There are four strong cross-peaks in the region ca. 2.83–3.48 ppm, stemming form the four non-equivalent SCH_2 protons, as well as the expected four absorptions from the individual olefinic protons of the 1,5-COD ligand. All of these coupling constants are of the order of 2 Hz or less. The ca. 1–2 Hz interaction for the Rh(COD) moiety was known (and used for the measurement), but the rhodium coupling constants to the methylene groups of the P,S ligand were not known before the measurement. Clearly the spectrum shows even more contacts and although a guess for $^{x}J(^{103}Rh,^{1}H)$ (based on the Rh(COD) literature) was sufficient to produce the metal chemical shift, the observed result can be considered as having a number of bonuses (i.e., extra correlations which might be useful in the future).

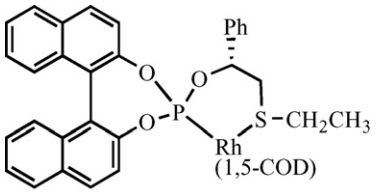

40

Fig. 19 shows the HMQC proton–tungsten correlation for the W(V1) imido-complex, **41** [48]. The *J*-value to the benzyl CH_2

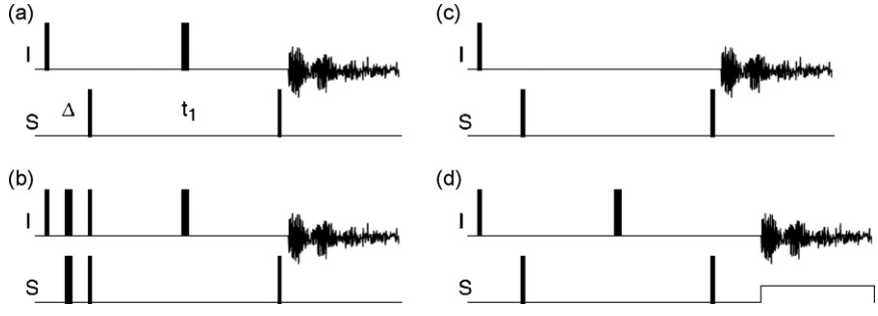

Fig. 17. Heteronuclear multiple quantum correlation (HMQC) pulse sequences. (a) Sequence for small *J*(I,S) values, (b) for larger, resolved *J*(I,S) values and phase sensitive presentation, (c) zero or double quantum variant for the determination of the I-spin-multiplicity, and (d) with refocussing and optional S-spin decoupling.

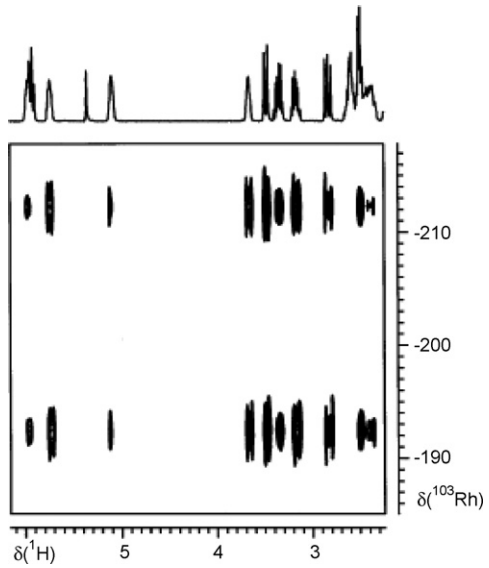

Fig. 18. HMQC ^{103}Rh spectrum for **40** showing the numerous contacts due to the various J(^{103}Rh,^{1}H) spin–spin interactions. The separation of the two horizontal cross-peaks represents ^{1}J(^{103}Rh,^{31}P) [47].

group (correlation not shown) was used for the measurement. However, it can be seen that the ^{183}W spin–spin couples not only through four bonds to the *ortho* but also through six bonds to the *para* protons of the imido-phenyl group. This was the first report of such long-range aryl-proton–tungsten interactions. These coupling constants to the protons of the phenyl group are less than 1 Hz, and their observation came as somewhat of a surprise.

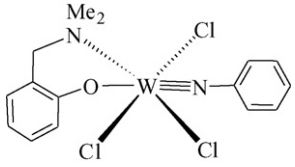

41

Any reasonable literature based estimate of the ^{183}W,^{1}H spin–spin coupling gives the spectrum with its metal chemical shift, and again there is a bonus: one could have used the much smaller tungsten-proton interaction. Indeed, in both examples, **40** and **41**, a guess for ^{x}J(M,^{1}H) which was incorrect by more than 100%, would have resulted in an observed spectrum due to the presence of several other, not previously recognized, coupling constants. One can consider that the HMQC is a "forgiving" method as it allows for a range of choice for *J*, while still performing sufficiently.

Although not immediately obvious (and certainly not relevant for these two examples), this chemical shift information comes at the cost of some selectivity, i.e., there can be *too many* interactions due to the various metal–proton coupling constants and, for every nucleus, this is not always desirable. For ^{31}P,^{1}H correlations, it is often important to limit the number of observed connectivities in order to (a) be certain of an assignment, (b) utilize their relative intensities and (c) find hidden resonances. A Pd-BINAP example is illustrative.[1]

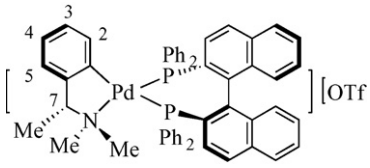

42

Fig. 20 shows two ^{31}P,^{1}H correlations for the cyclometallated BINAP Pd-complex **42** [49a]. The bottom trace was obtained via a ^{31}P,^{1}H-COSY and the top trace from an HMQC measurement. In the HMQC version one finds 8 or more contacts for each of the two non-equivalent ^{31}P signals and it is not simple to assign these cross-peaks based solely on their relative intensities. Admittedly, an interesting four-bond contact to the methine proton, H7, and other long-range interactions with H2 and H3 are visible. Further, these long-range P,H coupling constants are not all obvious from the 1D proton spectrum and, although they may have potential value, they are not immediately helpful. In the ^{31}P,^{1}H-COSY spectrum there are *fewer* contacts and these are (mostly) restricted to the three-bond interactions. In contrast to the situation for **40** or **41**, where one is attempting to measure the metal chemical shift, the ^{31}P chemical shift is not difficult to obtain. Rather one is using this correlation as a form of filter through which one can make assignments and occasionally find hidden (overlapped) resonances. If one is seeking to assign the specific P-phenyl protons (e.g., in order that they may be used as NOE probes), generally, one is better served by the ^{31}P,^{1}H-COSY spectrum [50].

Normally, there are no special problems associated with ^{13}C,^{1}H HMQC correlations. The assumption is made that ^{3}J(^{13}C,^{1}H) is larger than ^{2}J(^{13}C,^{1}H) and this is often correct [31]. Not surprisingly, given the discussion above, one often finds correlations due to the three-and-two–bond interactions, and provided that the proton assignment is clear, these can be helpful. Sometimes, relatively little is clear *until* the HMQC ^{13}C,^{1}H spectrum has been measured.

Fig. 21 shows the ^{13}C,^{1}H HMQC correlation for **43**, one of the complexes in which the BINAP is a 6e donor [12].

[1] This example is complicated by the dynamics [49b] associated with the restricted rotation of several of the P (phenyl) rings. Not all of the various proton signals are visible at room temperature. Nevertheless, the two spectra are sufficiently different to be informative.

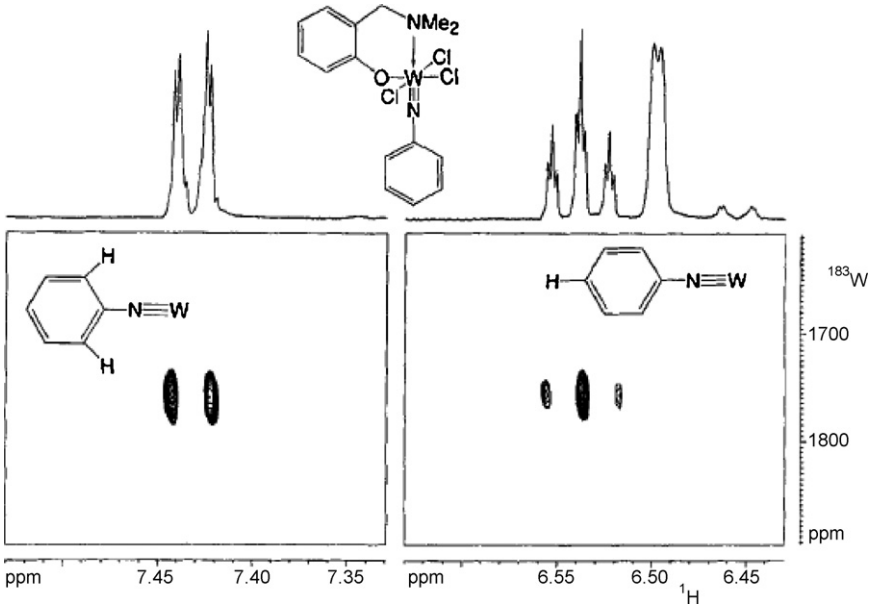

Fig. 19. Sections of the 11.7 T ^{183}W,^{1}H correlation for **41**. Note the cross-peaks to the remote *para* protons.

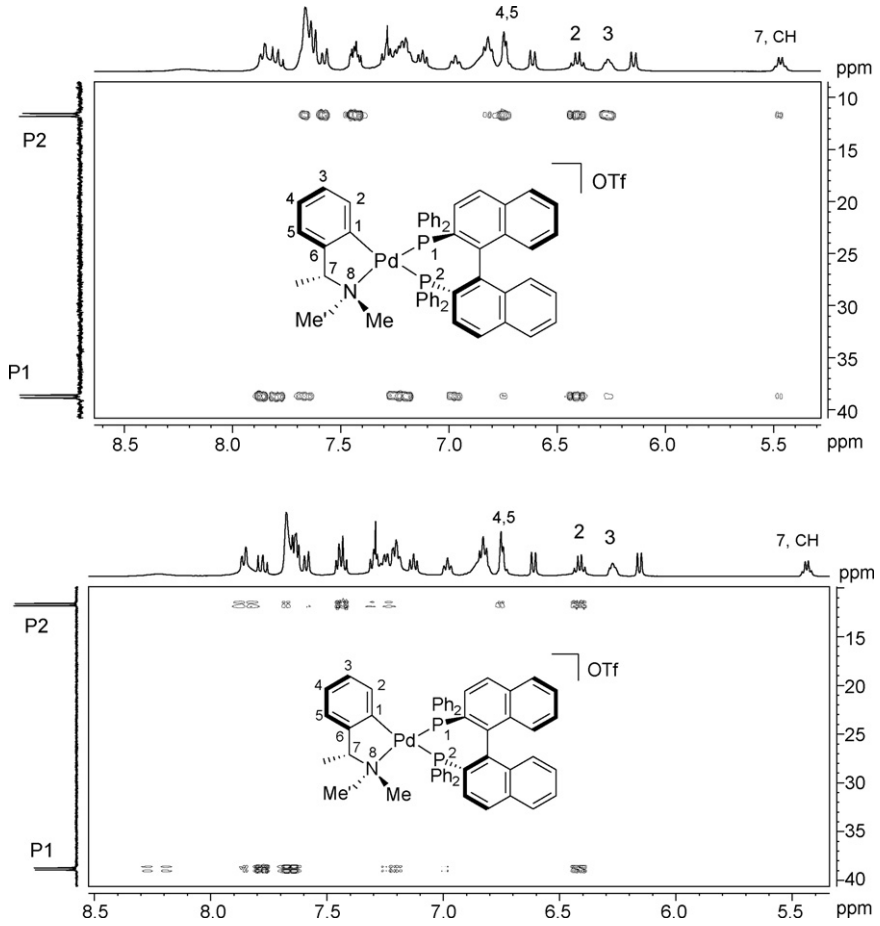

Fig. 20. ^{31}P,^{1}H HMQC (top) and ^{31}P,^{1}H COSY (below) for **42** at ambient temperature [48].

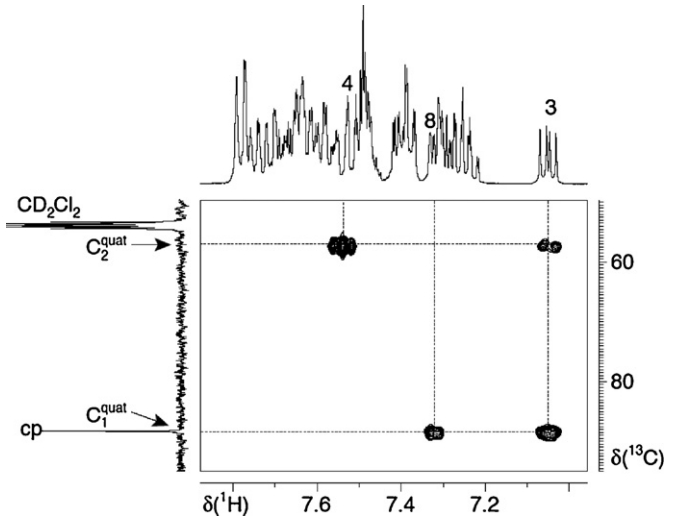

Fig. 21. HMQC $^{13}C,^{1}H$ correlation for **43**, revealing the η^2 binding mode of the olefin of BINAP to Ru(II) [12]. The conventional 1D ^{13}C signals are not visible, but the cross-peaks clearly indicate the ^{13}C chemical shifts for the two fully substituted carbon signals (optimized on $J(C–H) = 8$ Hz).

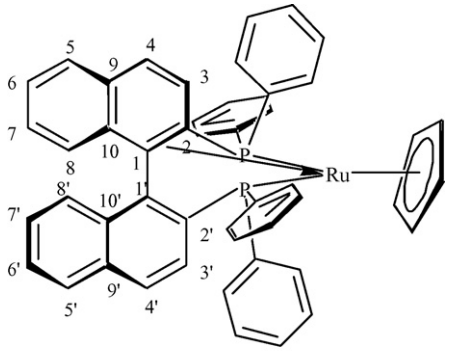

43

The proton assignment is anything but trivial and there was not enough signal-to-noise in the conventional 1D ^{13}C spectrum to unambiguously find the fully substituted carbon resonances for C1 and C2. Moreover, (as it develops) C1 is partially overlapped by the signal for the Cp ligand. Nevertheless, the $^{13}C,^{1}H$ HMQC correlation (which affords much better signal-to-noise than the 1D variant) readily reveals the fairly strong cross-peaks for the two sought after carbon resonances, via $^{3}J(^{13}C,^{1}H)$ and $^{2}J(^{13}C,^{1}H)$ interactions. The protons H3 (which, via the three-bond coupling, can be assigned with the help of a $^{31}P,^{1}H$-COSY spectrum) and H4 (assigned from the proton COSY, once one knows H3) give strong cross-peaks and clearly indicate the chemical shifts of the two crucial carbon signals. Both signals are shifted markedly to lower frequency in keeping with olefin complexation. Although not emphasized in this presentation, this example serves to illustrate the very significant sensitivity gain associated with the ^{13}C HMQC methodology. This should not be overlooked when deciding how to measure a dilute solution of a material whose ^{13}C signals are not easy to find. This is clearly a most useful NMR tool.

7. Concluding remarks

Returning to the chemistry, it is interesting that several P–C bonds in these Ru-biaryl phosphine complexes are readily cleaved, especially as many of the reactions indicated above take place under relatively mild conditions. Mechanistically speaking it is likely that, after complexation of a proximate biaryl double bond (see **34** and Scheme 4), the molecule is strained by the formation of the four-membered ring and this is confirmed by the solid-state X-ray studies. P–C bond breaking represents one way to relieve the strain. As the Ru-atom is already attached to the backbone π-system, via the olefin complexation, it need only "shift" slightly to coordinate two more double bonds and attain the stable η^6-arene complexation mode. The available acid proton binds the backbone arene carbon while the oxygen of either the acetate or water can attack the P-atom (see **36** and **39**). Once the complexed P-donor is bound to an oxygen atom, it represents a much more electrophilic site and the remaining P–C cleavage reactions become easier.

The ability to readily recognize these unexpected transformations stems from (a) the marked changes in the ^{31}P chemical shifts, (b) the ability to monitor the number of phenyl rings on the P-atom ($^{31}P,^{1}H$ correlation) and (c) the characteristic ^{13}C chemical shifts associated with olefin and/or arene complexation ($^{13}C,^{1}H$ correlation). All of these NMR measurements are currently of a fairly routine nature [51] (although not necessarily routinely carried out), and the modest amount of extra effort required is more than compensated by the additional insight they provide.

Acknowledgements

P.S.P. thanks the Swiss National Science Foundation, the "Bundesamt für Bildung und Wissenschaft" and the ETHZ for financial support, as well as Johnson Matthey for the loan of precious metals.

References

[1] P.S. Pregosin, R.W. Kunz, in: P. Diehl, E. Fluck, R. Kosfeld (Eds.), ^{31}P and ^{13}C NMR of Transition Metal Phosphine Complexes, vol. 16, Springer Verlag, 1976; in: L.D. Quin, J.G.Verkade (Eds.), Phosphorus-31 NMR Spectral Properties in Compound Characterization and Structural Analysis, VCH, New York, 1994.
[2] P.S. Pregosin, R. Salzmann, Coord. Chem. Rev. 155 (1996) 35; T. Branda, E.J. Cabrita, S. Berger, Prog. Nucl. Magn. Reson. Spectrosc. 46 (2005) 159.
[3] P. Pregosin, in: L.D. Quin, J.G. Verkade (Eds.), Methods in Stereochemical Analysis, vol. 8, VCH, Deerfield Beach Fla., 1987, p. 465.
[4] P.S. Pregosin, H. Ruegger, in: J. McCleverty, T.J. Meyer (Eds.), Comprehensive Coordination Chemistry, vol. II, Elsevier, Amsterdam, 2003, p. 1.
[5] R. Hermatschweiler, P.S. Pregosin, A. Albinati, Inorg. Chim. Acta 354 (2003) 90.
[6] N. Feiken, P.S. Pregosin, G. Trabesinger, Organometallics 16 (1997) 3735.
[7] M. Bennett, A.K. Smith, J. Chem. Soc., Dalton (1974) 233;
M.A. Bennett, I.J. McMahon, S. Pelling, M. Brookhart, D.M. Lincoln, Organometallics 11 (1992) 127;
M.A. Bennett, Z. Lu, X. Wang, M. Brown, D.C.R. Hockless, J. Am. Chem. Soc. 120 (1998) 10409.

[8] H. Caldwell, P.S. Pregosin, J. Organomet. Chem. 692 (2007) 4043.
[9] N. Feiken, P.S. Pregosin, G. Trabesinger, M. Scalone, Organometallics 16 (1997) 537.
[10] B.E. Mann, B.F. Taylor, ^{13}C NMR Data for Organometallic Compounds, Academic Press, London, 1981.
[11] T.D.W. Claridge, Tetrahedron Organic Chemistry, vol. 19, Elsevier Science Ltd., 1999 (see also Ref. [31]).
[12] N. Feiken, P.S. Pregosin, G. Trabesinger, A. Albinati, G.L. Evoli, Organometallics 16 (1997) 5756.
[13] T. Cheng, D.J. Szalda, R.M. Bullock, Chem. Commun. (1999) 1629.
[14] (a) H. Aneetha, M. Jemenez-Tenorio, M. Carmen Puerta, P. Valerga, K. Mereiter, Organometallics 21 (2002) 628, see also;
(b) C.W. Cyr, S.J. Rettig, B.O. Patrick, B.R. James, Organometallics 21 (2002) 4672;
(c) X.P. Wang, X. Li, J. Sun, K. Ding, Organometallics 22 (2003) 1856;
(d) J.L. Snelgrove, J.C. Conrad, M.D. Eelman, M.M. Moriarty, G.P.A. Yap, D.E. Fogg, Organometallics 24 (2005) 103.
[15] (a) S. Doherty, C.R. Newman, C. Hardacre, M. Nieuwenhuyzen, J.G. Knight, Organometallics 22 (2003) 1452;
(b) J.L. Becker, P.S. White, M.R. Gagne, Organometallics 22 (2003) 3245.
[16] T.J. Geldbach, P.S. Pregosin, A. Albinati, Organometallics 22 (2003) 1443.
[17] T.J. Geldbach, P.S. Pregosin, S. Rizzato, A. Albinati, Inorg. Chim. Acta 359 (2006) 962.
[18] D.D. Pathak, H. Adams, N.A. Bailey, P.J. King, C. White, J. Organomet. Chem. 479 (1994) 237.
[19] C.J. den Reijer, P. Dotta, P.S. Pregosin, A. Albinati, Can. J. Chem. 79 (2001) 693.
[20] T. Hayashi, J. Syn. Org. Chem. Jpn. 52 (1994) 900.
[21] T. Hayashi, H. Iwamura, Y. Uozumi, Y. Matsumoto, F. Ozawa, Synthesis-Stuttgart (1994) 526.
[22] Y. Uozumi, K. Kitayama, T. Hayashi, K. Yanagi, E. Fukuyo, Bull. Chem. Soc. Jpn. 68 (1995) 713.
[23] T. Hayashi, M. Kawatsura, Y. Uozumi, J. Am. Chem. Soc. 120 (1998) 1681.
[24] P. Dotta, P.G. Anil Kumar, P.S. Pregosin, A. Albinati, S. Rizzato, Organometallics 23 (18) (2004) 4247.
[25] P. Leoni, M. Pasquali, M. Sommovigo, A. Albinati, F. Lianza, P.S. Pregosin, H. Ruegger, Organometallics 12 (1993) 4503.
[26] Christmann, D.A. Pantazis, J. Benet-Buchholz, J.E. McGrady, F. Maseras, R. Vilar, Organometallics 25 (2006) 5990.
[27] T. Murahashi, M. Fujimoto, M. Oka, Y. Hashimoto, T. Uemura, Y. Tatsumi, Y. Nakao, A. Ikeda, S. Sakaki, H. Kurosawa, Science 313 (2006) 1104.
[28] T. Murahashi, T. Uemura, H. Kurosawa, J. Am. Chem. Soc. 125 (2003) 8436;
T. Murahashi, T. Nagai, T. Okuno, T. Matsutani, H. Kurosawa, Chem. Commun. (2000) 1689.
[29] P. Dotta, P.G.A. Kumar, P.S. Pregosin, A. Albinati, S. Rizzato, Organometallics 22 (2003) 5345.
[30] P. Garrou, Inorg. Chem. 14 (1975) 1435.
[31] H. Kalinowski, S. Berger, S. Braun, ^{13}C NMR Spektroskopie, Georg Thieme, Stuttgart, 1984.
[32] P.G.A. Kumar, P. Dotta, R. Hermatschweiler, P.S. Pregosin, A. Albinati, S. Rizzato, Organometallics 24 (2005) 1306.
[33] M. Soleilhavoup, L. Viau, G. Commenges, C. Lepetit, R. Chauvin, Eur. J. Inorg. Chem. (2003) 207.
[34] G.C. Lloyd-Jones, S.C. Stephen, M. Murray, C.P. Butts, S. Vyskocil, P. Kocovsky, Chem. Eur. J. 6 (2000) 4348.
[35] P. Kocovsky, S. Vyskocil, I. Cisarova, J. Sejbal, I. Tislerova, M. Smrcina, G.C. Lloyd-Jones, S.C. Stephen, C.P. Butts, M. Murray, V. Langer, J. Am. Chem. Soc. 121 (1999) 7714; for another bonding variation see also J.W. Faller, N. Sarantopoulos, Organometallics 23 (2004) 2008. Some Pd-η^3-benzyl complexes have related structures: see K.K. Hii, T.D.W. Claridge, R. Giernoth, J.M. Brown, Adv. Syn. Catal. 346 (2004) 983 and references therein.
[36] D. Huber, P.G.A. Kumar, P.S. Pregosin, A. Mezzetti, Organometallics 24 (2005) 5221;
D. Huber, P.G.A. Kumar, P.S. Pregosin, I.S. Mikhel, A. Mezzetti, Helv. Chim. Acta 89 (2006) 1696, however see;
N.M. Brunkan, P.S. White, M.R. Gange, J. Am. Chem. Soc. 120 (1998) 11002 (for a related binol complex).
[37] C.J. den Reijer, H. Rueger, P.S. Pregosin, Organometallics 17 (1998) 5213.
[38] C.J. den Reijer, M. Worle, P.S. Pregosin, Organometallics 19 (2000) 309.
[39] T.J. Geldbach, C.J. den Reijer, M. Worle, P.S. Pregosin, Inorg. Chim. Acta 330 (2002) 155.
[40] T.J. Geldbach, D. Drago, P.S. Pregosin, Chem. Commun. (2000) 1629.
[41] T.J. Geldbach, P.S. Pregosin, A. Albinati, F. Rominger, Organometallics 20 (2001) 1932.
[42] W. von Philipsborn, Pure Appl. Chem. 58 (1986) 513;
W. von Philipsborn, Chem. Soc. Rev. 28 (1999) 95.
[43] D. Nanz, W. von Philipsborn, J. Mag. Res. 92 (1991) 560.
[44] B.R. Bender, M. Koller, D. Nanz, W. von Philipsborn, J. Am. Chem. Soc. 115 (1993) 5889.
[45] B.T. Heaton, J.A. Iggo, I.S. Podkorytov, D.J. Smawfield, S.P. Tunik, R. Whyman, J. Chem. Soc., Dalton Trans. (1999) 1917.
[46] J.J. Templeton, C.C. Philipp, P.S. Pregosin, H. Rüegger, Magn. Reson. Chem. 31 (1993) 58.
[47] A. Albinati, J. Eckert, P.S. Pregosin, H. Rüegger, R. Salzmann, C. Stössel, Organometallics 16 (1997) 579.
[48] A. Macchioni, P.S. Pregosin, H. Ruegger, G. van Koten, P.A. van der Schaaf, R.A.T.M. Abbenhuis, Magn. Reson. Chem. 32 (1994) 235.
[49] (a) D. Nama, P. Butti, P.S. Pregosin, unpublished results;;
(b) Restricted rotation in complexes of BINAP and biaryl phosphines is well known: see;
P. Dotta, P.G.A. Kumar, P.S. Pregosin, A. Albinati, S. Rizzato, Organometallics 23 (2004) 2295, and;
D. Nama, D. Schott, P.S. Pregosin, L.F. Veiros, M.J. Calhorda, Organometallics 25 (2006) 4596.
[50] V. Sklenar, H. Miyashiro, G. Zon, H.T. Miles, A. Bax, FEBS 208 (1986) 94.
[51] A. Schmid, H. Piotrowski, T. Lindel, Eur. J. Inorg. Chem. (2003) 2255, in the characterization of their Ru(Cp*)(arene) salts, imply that these measurements are standard.